ELSEVIER

Polymer 43 (2002) 6019–6025

polymer

www.elsevier.com/locate/polymer

A DFT study of polymerization mechanisms of indole

Mine Yurtsever[a], Ersin Yurtsever[b,*]

[a]*Department of Chemistry, Istanbul Tech. University, Maslak, Istanbul 80626, Turkey*
[b]*Department of Chemistry, Koc University, Rumeli Feneri Yolu, Sarıyer, Istanbul 80910, Turkey*

Received 2 May 2002; received in revised form 30 July 2002; accepted 30 July 2002

Abstract

Polymerization of unsubstituted indoles is studied by accurate density functional theory calculations. Relative stability of all possible dimers of indole is computed in order to understand the thermodynamics of polymerization. It is observed that 2-position is the most likely site to enhance polymerization. A selected set of trimers and tetramers which use a 2-position for linkages are generated to understand the further growth of polyindole. A study of local minima arising from different distributions of the torsional angles reveals that there are two equally probable conformations and the one with the torsional angle changing signs alternatively is slightly favored. The cyclic structures are also investigated and it is shown that it is possible to generate stable three- and four-membered cyclic structures. Finally, the structures of radical cations and intermediate states are fully optimized and the energetics of these metastable species are used to explain the competing mechanisms of radical–radical and radical–neutral pathways. © 2002 Published by Elsevier Science Ltd.

Keywords: Density functional theory; Indole; Polymerization

1. Introduction

N-containing heteroaromatic organic molecules have very interesting properties. The chemical or electrochemical oxidation of these molecules yields conducting polymers that could find an enormous amount of applications especially in the electronics as new materials. Polyindole has air stability and its conductivity is about 10^{-3}–10^{-1} S/cm depending upon the synthesis technique and the nature of dopant ions. It is usually obtained by the anodic oxidation of indole under suitable conditions [1]. The polymerization efficiency and the conductivity of polyindole are lower than the other known N-containing conducting polymers so initially it did not attract much attention as the other types of conducting materials. One of the reasons for this behavior is the large number of polymerization schemes. Majority of these coupling schemes result in various forms of branching and large deviations from planarity. Like most of the conjugated polymers such as polythiophenes and polypyrroles, these branchings and defects create highly complex structures that are difficult to analyze with standard spectroscopic techniques. The heavy dose of different coupling forms leads to much shorter conjugation lengths and consecutively reduced conductivity. Hence, synthesis techniques that generate regioselective structures become extremely important.

In order to analyze the polymerization mechanism of indole, several spectroscopic and theoretical calculations have been carried out. As most likely coupling sites, 1 and 3 positions [1–3], 3–6 positions [4], 2–3 positions [5,6] and 3–3, 2–2 couplings [7] were suggested. Although recent semi-empirical theoretical calculations were indicating 2 and 3 positions of the monomer as the most likely coupling sites, the level of theory used was not adequate to explain the complexity of the processes, and more accurate calculations are required.

Another interesting and somewhat unresolved issue is the polymerization mechanism of conjugated polymers in general, and specifically in polyindoles. The stability of various intermediate structures generated during the oxidation has to be understood to investigate the competing mechanisms of radical–radical or radical–neutral pathways. The presence of various linkages between monomers makes this analysis more difficult. In the polymerization, radical cations are generated either by electron transfer within a charge transfer complex or by electrochemical means. Then the polymerization can proceed via the

* Corresponding author. Tel.: +90-2123381401; fax: +90-2123381559.
E-mail address: eyurtsev@ku.edu.tr (E. Yurtsever).

0032-3861/02/$ - see front matter © 2002 Published by Elsevier Science Ltd.
PII: S0032-3861(02)00510-4

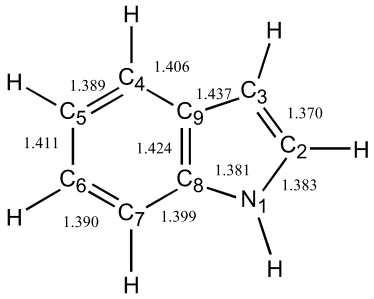

Fig. 1. Geometry of indole monomer.

coupling of radical cations with neutral species or with radical cations. The dominant reaction is said to be the one following a radical attack on neutral species [8]. The thermodynamics of these two processes can be studied by applying quantum mechanical methodology and analyzing each step in these processes individually. We have reported a similar approach for polypyrrole [9].

In this work, we present accurate density functional theory (DFT) calculations on both stable oligomers and metastable intermediates. We carry out a detailed study of the bonding in small oligomers so that extrapolations to the longer chains can be made [10–12]. Also the possibility of regular structures such as those symmetric linear oligomers or cyclic structures is discussed. Finally, we report computational results on the stability and structures of the possible intermediates to predict the relative probabilities of polymerization mechanisms which cannot be extracted from experimental data.

2. Method

The calculations are carried out with the GAUSSIAN 98 package [13]. DFT calculations are carried out using the three-parameter hybrid-functional of Becke [14]. Several basis sets are employed in calculations. The smallest basis set is the 3-21G, for energy calculations 6-31G(d) is used and for testing the basis size effects we have employed 6-311+G(2d,p). The smallest basis set allows us to optimize all the geometrical parameters of large oligomers. It is generally accepted that with 3-21G, the calculated bond lengths and angles are in good agreement with the experimental data. On the other hand, the energetics is usually more dependent on the basis set. We have also carried out full optimizations with 6-31G(d) on some structures and found out that relative trends are optimally obtained from 6-31G(d)//3-21G. A very accurate calculation using the G-311 + G(2d,p) on 6-31G(d) geometry did not give any different results. In Fig. 1, we present the optimum structure of the neutral monomer obtained with 6-31G(d) basis set. The molecule is planar, a high degree of conjugation is observed at all bond lengths with the possible

Table 1
Relative energy of indole dimers (kcal/mol)

	3-21G//3-21G	6-31G(d)//3-21G	6-31G(d)//6-31G(d)	6-311+G(2d,p)//6-31G(d)
11	34.14	32.69	32.45	35.39
12	7.84	8.81	8.85	10.64
13	8.84	10.23	10.25	11.93
14	8.19	9.04	9.06	10.64
15	8.65	9.20	9.21	10.76
16	8.54	9.09	9.02	10.66
17	7.80	9.03	9.02	10.53
22	0.00	0.00	0.00	0.00
23	2.10	1.88	1.95	2.15
24	2.62	2.53	2.54	2.64
25	3.21	2.65	2.64	2.59
26	2.96	2.43	2.40	2.48
27	1.45	1.39	1.39	1.69
33	5.23	4.27	4.33	4.44
34	6.07	5.23	5.29	5.39
35	6.48	5.65	5.63	5.55
36	6.07	5.19	5.16	5.14
37	3.75	4.05	3.99	4.06
44	7.07	6.60	6.58	6.26
45	7.17	6.66	6.57	6.26
46	6.89	6.28	6.23	5.96
47	5.24	5.27	5.25	5.11
55	7.33	6.57	6.55	6.28
56	7.02	6.24	6.18	5.97
57	5.60	5.55	5.53	5.35
66	6.76	5.93	5.82	5.77
67	5.16	5.07	5.04	4.98
77	3.39	3.94	3.87	3.92

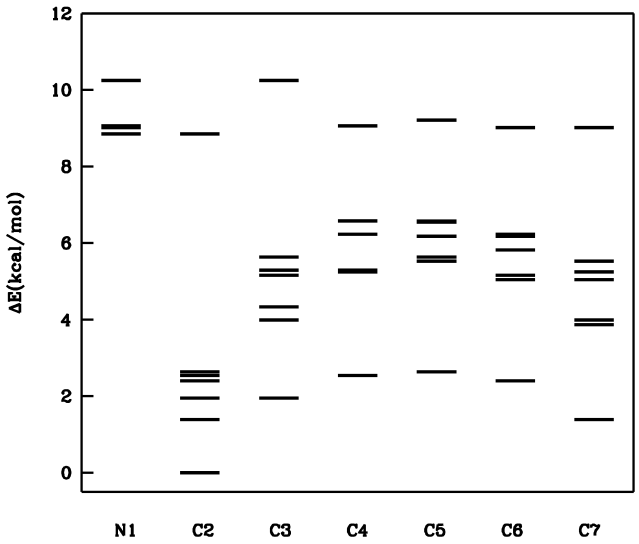

Fig. 2. Energetics of indole dimers.

exception of a pronounced double bond at C_2-C_3. The negative charge is mostly on N atom and the positive charge is localized again around C_2-C_3. The molecule has a relatively high dipole moment of 2.17 D.

3. Dimers

There are seven (atoms 1–7) possible sites on an indole molecule for growth and there are in terms altogether 28 linkage types in dimer. We denote these dimers as well as their larger oligomers with the notation (klmn); e.g. a trimer, where atom k of the first monomer and the atom l of the second monomer forms the first monomer–monomer linkage and so on. In Table 1, we present the energetics of these 28 dimers with DFT/3-21G//DFT/3-21G, DFT/6-31G(d)//DFT/3-21G, DFT/6-31G(d)//DFT/6-31G(d) and DFT/6-311+G(2d,p)//DFT/6-31G(d). The energy is reported relative to the lowest energy linkage of (22).

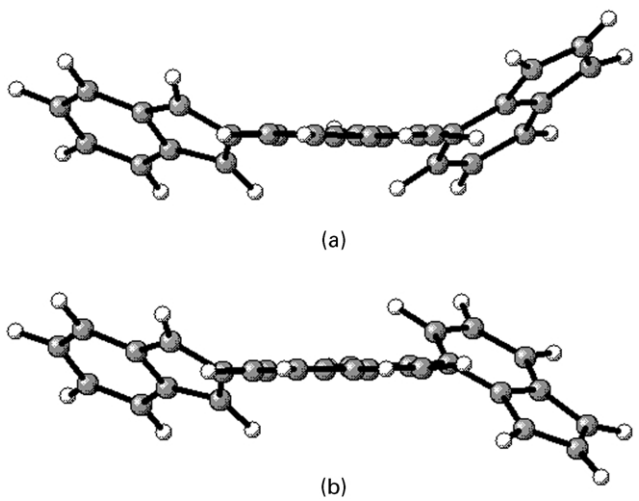

Fig. 3. (a) 2727_p; (b) 2727_s.

Table 2
Energetics of regioregular oligomers

Structure	Relative energy (kcal/mol)
Dimer	
23	0.56
24	1.15
25	1.26
26	1.01
27	0.00
Trimer	
2323_s	1.46
2323_p	2.42
2424_s	1.87
2424_p	1.98
2525_s	1.98
2525_p	2.07
2626_s	1.51
2626_p	1.56
2727_s	0.16
2727_p	0.00
Tetramer	
232323_s	4.07
242424_s	2.98
242424_p	2.53
252525_s	2.86
252525_p	2.95
262626_s	2.09
262626_p	2.15
272727_s	0.37
272727_p	0.00

By plotting these relative energy on an energy diagram (Fig. 2), we observe the following trends. The bonding from nitrogen atom is the least stable one. The most favorable linkage should invariably involve a 2-position. But it is clear that the lowest energy configuration of (22) does not allow further polymerization. Positions 3 and 7 are close to position 2 in terms of reactivity and positions 4–6 are less reactive. The geometry of these structures deviate from planarity to a great extent. There are general trends in describing shapes of dimers. For the case of N–N bridge, two monomers are perpendicular to each other. When only one N is involved for the dimerization process, the torsional angle changes from 45° to 65°. The variation of the torsional angles from 3-21G to 6-31G(d) is very small in the order of 2–3°. Dimer formation through a C_2 atom results in the small torsional angle, the smallest being around 20° for (22) and the others are around 30°. All other linkage types display torsional angles between 40° and 50°. The monomer–monomer distance has the shortest value for N–N bridge with 1.37 Å. Those dimers involving N have distances around 1.42–1.44 Å and all others are around 1.47–1.49 Å except for (22) which is 1.44 Å.

Additional single point energy calculations are carried out with DFT/6-311+G(2d,p)//DFT/6-31g(d). The ordering of the relative energy of dimers with smaller basis calculations agrees extremely well with the highly accurate

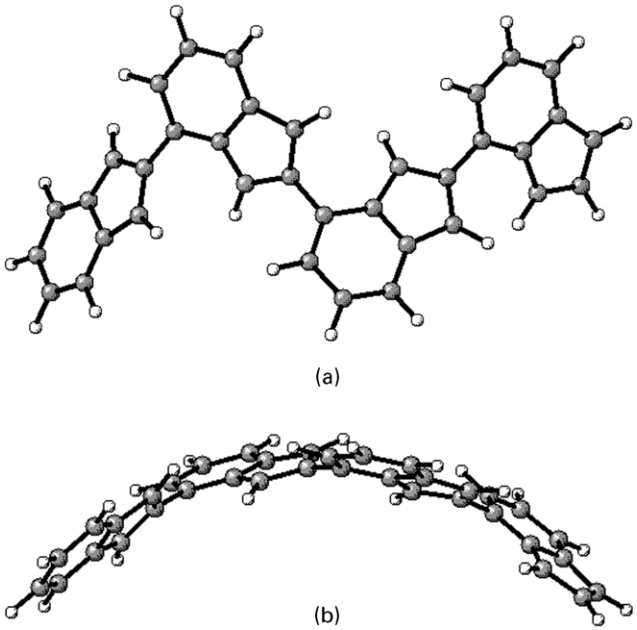

Fig. 4. (a) 272727_s; (b) 272727_p.

ones. The correlation coefficient between the results of this basis and DFT/6-31G(d)//DFT/3-21G is 0.996.

4. Trimers and tetramers

The number of possibilities for larger oligomers increases almost exponentially. For example there are over 1000 possibilities for the trimer. Instead of searching all possibilities, we proceed to study those oligomers that are both energetically feasible and have some regioregularity. From the study of dimers, it is clear that growth via C_2 is thermodynamically the most important one. (22) is excluded as it does not allow further growth, hence repetitive additions through (23)–(27) are considered. Since the torsional angles impose strong restrictions on growth processes, we have computed two types of structures (definition of the torsional angle requires four atoms. For (*mn*) dimer, they are in the order of atoms $(m-1)$, m of the first monomer and n, $(n+1)$ of the second monomer. The numbering of atoms are clockwise starting from N as shown in Fig. 1). The first one is denoted by a suffix (_s) and here the torsional angles between successive monomers increase monotonically generating spiraling structures. In the other case (_p), torsional angles alternate in sign resulting in structures that are closer to planarity. In Fig. 3a and b optimum structures of these two forms for (2727) trimer are given.

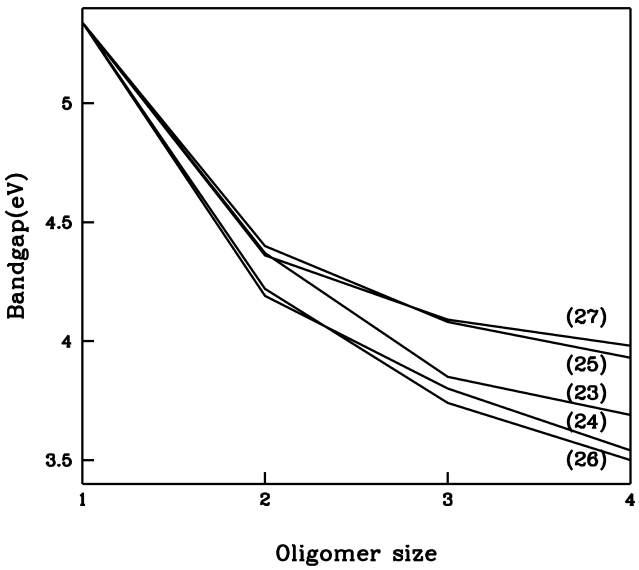

Fig. 5. Bandgap as a function of the oligomer size.

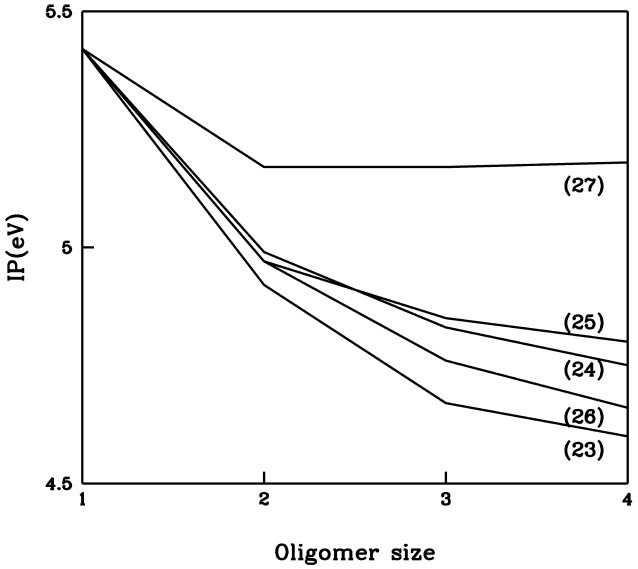

Fig. 6. First ionization potential as a function of the oligomer size.

In Table 2, we present the energetics of such regioregular structures. For all cases studied bonding through (27) linkages are the most stable ones. p-Isomer is always more stable with torsional angles between successive monomers remaining constant around 35°. Optimum structures for both trimer and the tetramer of the p-isomer show the formation of a linear chain with a pronounced curvature (Fig. 4a and b). The charges on heavy atoms show that the electron density shifts towards the linked atoms (2 and 7) from positions 1, 3, 6 and 8. The positions 4, 5, and 9 are unaffected by the growth process. The bandgap and the first ionization potentials of these structures are given in Figs. 5 and 6. Even though, the actual conductivity mechanisms of conjugated polymers are open to serious debate, it is commonly accepted that the magnitude of the bandgap and similarly, the first ionization potential has some bearing on the probability of exciting electrons to higher orbitals. Here, we are interested in the convergence from single molecule properties (discrete spectrum) to long chain asymptote (band structure). The bandgap is reduced from 5.5 to 3.5 eV from monomer to the tetramer. The vertical ionization potential is reduced from 5.4 to 4.6–4.7 eV for all coupling

Table 3
Energetics of cyclic structures

Structures	Relative energy (kcal/mol)
Three-membered structure	
12	36.3
23	0.0
45	34.4
56	23.2
67	35.1
Four-membered structures	
12	158.8
23	0.0
45	262.1
56	27.7
67	19.6

types except (27), where the ionization potential remains constant around 5.2 eV. It is interesting to note that electronic properties of oligomers grown via (27) linkages behave almost identical after dimers, whereas the other regioregular structures require longer chains in order to have converged properties.

5. Cyclic structures

It has been reported that the possibility of a large number of coupling schemes may result in cyclic structures [15]. These are the undesired side products of the polymerization and they decrease the polymerization efficiency. We have tried to find out whether these structures are sterically and thermodynamically stable. It turns out that it is possible to generate cyclic structures from three and four monomers with the linkage types (12), (23), (45), (56) and (67). Energetics of these oligomers are given in Table 3. The

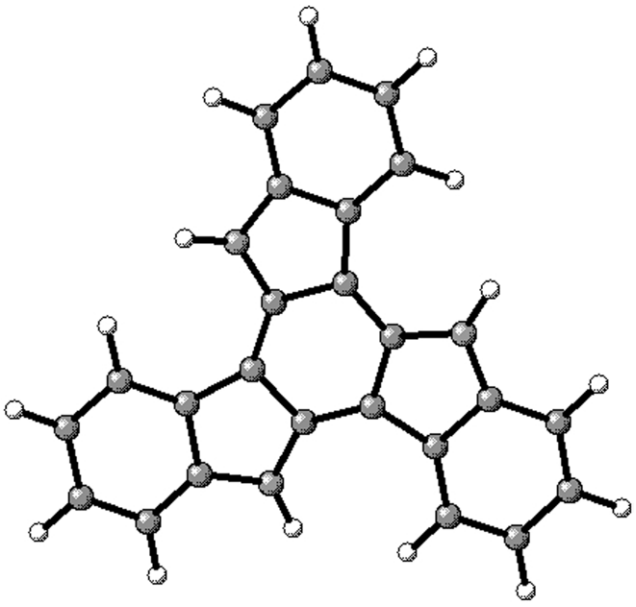

Fig. 7. Three-membered cyclic structure via 23 linkage.

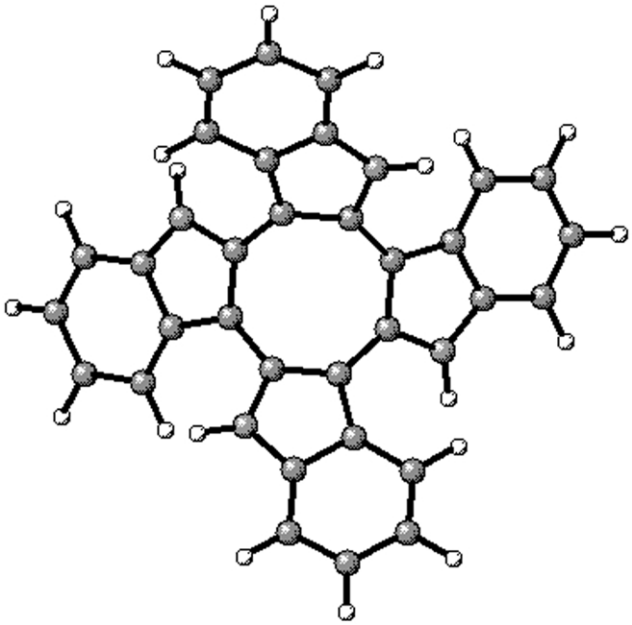

Fig. 8. Four-membered cyclic structure via 23 linkage.

three-monomer structures are all planar (Fig. 7), they belong to C_{3h} symmetry group and form a six-membered ring at the center. When the bonding is through the five-membered rings of indole, the monomer–monomer bond lengths are shorter than those are in the monomers; however, if the six-membered rings are connected this trend is reversed. On the other hand, stable four-monomer structures deviate from planarity to a great extent, they belong to C_{2v} symmetry group (Fig. 8). An eight-membered ring is formed at the

Table 4
Bond lengths and charges on atoms for neutral, singly charged and doubly charged indole

Bond lengths (Å)	M	M^+	M^{++}
N_1–C_2	1.383	1.337	1.303
C_2–C_3	1.370	1.424	1.491
C_3–C_9	1.437	1.407	1.372
C_9–C_4	1.406	1.418	1.449
C_4–C_5	1.389	1.397	1.394
C_5–C_6	1.411	1.397	1.398
C_6–C_7	1.390	1.424	1.466
C_7–C_8	1.399	1.374	1.354
C_8–C_9	1.424	1.427	1.440
C_8–N_1	1.381	1.408	1.438
Charges summed up with H (a.u.)			
N_1	−0.35	−0.22	−0.11
C_2	0.20	0.39	0.56
C_3	−0.10	0.05	0.18
C_4	−0.08	0.07	0.25
C_5	−0.02	0.09	0.19
C_6	−0.03	0.10	0.25
C_7	−0.04	0.08	0.20
C_8	0.31	0.32	0.34
C_9	0.12	0.13	0.14

Route 1

$M \longrightarrow M^{+\cdot} + e^-$

$M^{+\bullet} + M \longrightarrow M_2^{+\bullet}$

$M_2^{+\bullet} \longrightarrow M_2^{+2} + e^-$

$M_2^{+2} \longrightarrow M_2 + 2H^+$

Route 2

$M \longrightarrow M^{+\bullet} + e^-$

$M^{+\bullet} + M^{+\bullet} \longrightarrow M_2^{++}$

$M_2^{+2} \longrightarrow M_2 + 2H^+$

Scheme 1. Two routes of polymerization. M: monomer; $M^{+\cdot}$: radical cation.

center that has a strong boat-like structure. In all cases, the cyclic formation using (23) bridges are the most stable ones, whereas the (12) and (45) being highly unstable. (56) and (67) linkages also form reasonably stable structures.

6. Growth mechanism

The structural changes of indoles upon oxidation is summarized in Table 4. Upon oxidation, there are some significant changes in the geometry of the monomer. The neutral monomer has a high degree of conjugation, whereas the oxidized forms, especially the doubly charged one display pronounced single and double bonds. C_2-C_3 and C_6-C_7 bonds which have strong double bond character in the neutral indole extend and are converted into single bonds. Conversely, $N-C_2$, C_3-C_9 and C_7-C_8 gain double bond character. $C_8-C_9-C_4-C_5$ sequence is primarily unaffected by the oxidation. The changes in the charge distribution show similar trends. Upon ionization, the additional charges are distributed to all atoms except C_8 and C_9. N remains the only negatively charged atom in M^{++}, and C_2 is the most electropositive site.

The polymerization may proceed via two different paths (Scheme 1). Each starts with the formation of cationic radical. For simplicity we will describe the dimer formation. The spin density of the radical shows that the radical is mainly formed in the pyrrolic moiety. This radical may attack a neutral monomer (Route 1) forming a radical dimer, which then is oxidized once more. The doubly charged ion then releases two protons to form the neutral dimer. In the other pathway (Route 2), radical attack another radical which then forms the dimer by releasing two protons again.

In order to understand the thermodynamics of each route, we have optimized structures of singly and doubly charged cations for linkage types (23)–(27). The basic characteristics of these ions can be summarized as: both monomers retain their planar structures. If one molecule lies in the $x-y$ plane, the other monomer lies parallel to it at $z = z_0$, where z_0 is around 2.9 Å for the singly charged and around 1.6 Å for the doubly charged species. The molecular axes are perpendicular to each other (Fig. 9). Protons that are released at the next step have torsional angles of 60° with respect to monomer planes.

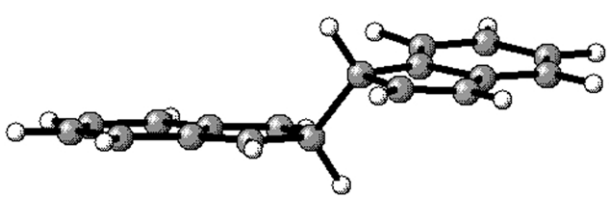

Fig. 9. Structure of the intermediate (doubly charged dimer with 23 linkage).

Table 5
Reaction energies for growth steps (kcal/mol)

Step	(23)	(24)	(25)	(26)	(27)
$M \rightarrow M^+$	167.6	167.6	167.6	167.6	167.6
Route 1					
$M + M^+ \rightarrow D^+$	−16.1	−15.6	−15.6	−15.4	−15.6
$D^+ \rightarrow D^{++}$	229.9	229.4	229.7	227.4	237.8
Route 2					
$M{+}{+}M^+ \rightarrow D^{++}$	40.1	46.2	46.5	44.4	54.7
$D^{++} \rightarrow D$	368.4	363.0	362.7	364.7	353.3

In Table 5, ΔE of each step is given. After the radical is formed, the attack of the radical on the neutral monomer in Route 1 is exothermic; however, the second ionization is very high in the order of 230 kcal/mol. Route 2 involves one more radical formation (167 kcal/mol) and the D^{++} formation which is in the order of 50 kcal/mol. The comparison of these two routes shows that the rate determining step is the second ionization of the intermediate which makes the radical–radical pathway more likely to take place. The complete procedure is relatively independent of the type of linkages involved in the dimerization.

7. Conclusions

We have presented an accurate and extensive DFT study of the structures and energetics of indole oligomers. We believe that polymerization goes through forming bonds between C_2 and another atom, more preferably C_7. The regioregular structures should show relatively high stability and their synthesis may be possible especially some of the sites such as C_3 are blocked by proper substitutions. By such substitutions it is also possible to prevent formation of stable cyclic structures. The mechanism is more likely to occur via a radical–radical pathway.

References

[1] Waltman RY, Diaz AF, Bargon J. J Phys Chem 1984;88:4343–6.
[2] Choi KM, Kim CY, Kim KH. J Phys Chem 1992;96:3782–8.
[3] Choi KM, Jang JH, Rhee H, Kim KH. J Appl Polym Sci 1992;46:1695–706.
[4] Koleli F, Saglam M, Turut A, Efeoglu H. Tr J Chem 1994;18:22–7.
[5] Zotti G, Zecchin S, Schiavon G, Seraglia R, Berlin A, Canavesi A. Chem Mater 1994;6:1742–8.
[6] Talbi H, Monard G, Loos M, Billaud D. Theochem 1998;434:129–34.
[7] Saraji M, Bagheri A. Synth Met 1988;98:57–63.
[8] Talbi H, Monard G, Loos M, Billaud D. Synth Met 1999;101:115–6.

[9] Yurtsever E. Synth Met 2001;119:227–8.
[10] Yurtsever M, Yurtsever E. Synth Met 1999;98:221–7.
[11] Yurtsever E, Esentürk O, Pamuk HÖ, Yurtsever M. Synth Met 1999; 98:229–36.
[12] Yurtsever M, Yurtsever E. J Phys Chem A 2000;104:362–9.
[13] Frisch MJ, Trucks GW, Schlegel HB, Scuseria GE, Robb MA, Cheeseman JR, Zakrzewski VG, Montgomery Jr. JA, Stratmann RE, Burant JC, Dapprich S, Millam JM, Daniels AD, Kudin KN, Strain MC, Farkas O, Tomasi J, Barone V, Cossi M, Cammi R, Mennucci B, Pomelli C, Adamo C, Clifford S, Ochterski J, Petersson GA, Ayala PY, Cui Q, Morokuma K, Malick DK, Rabuck AD, Raghavachari K, Foresman JB, Cioslowski J, Ortiz JV, Stefanov BB, Liu G, Liashenko A, Piskorz P, Komaromi I, Gomperts R, Martin RL, Fox DJ, Keith T, Al-Laham MA, Peng CY, Nanayakkara A, Gonzalez C, Challacombe M, Gill PMW, Johnson B, Chen W, Wong MW, Andres JL, Gonzalez C, Head-Gordon M, Replogle ES, Pople JA. GAUSSIAN 98, Revision A.6. Pittsburgh, PA: Gaussian, Inc., 1998.
[14] Becke AD. J Chem Phys 1996;104:1040–6.
[15] Mount AR, Thomson AD. J Chem Soc, Faraday Trans 1998;94: 553–8.